γ-ray spectroscopy of low-lying excited states and shape competition in ^{194}Os

T. Daniel,[1,2,*] S. Kisyov,[3] P. H. Regan,[1,4] N. Marginean,[3] Zs. Podolyák,[1] R. Marginean,[3] K. Nomura,[5,6] M. Rudigier,[1] R. Mihai,[3] V. Werner,[7] R. J. Carroll,[1] L. A. Gurgi,[1] A. Oprea,[3] T. Berry,[1] A. Serban,[3,8] C. R. Nita,[3] C. Sotty,[3] R. Suvaila,[3] A. Turturica,[3] C. Costache,[3] L. Stan,[3] A. Olacel,[3] M. Boromiza,[3,8] and S. Toma[3]

[1]*Department of Physics, University of Surrey, Guildford GU2 7XH, United Kingdom*
[2]*Department of Physics, Benue State University, PMB 102119, Makurdi, Nigeria*
[3]*Horia Hulubei National Institute of Physics and Nuclear Engineering (IFIN-HH), RO-077125 Bucharest, Romania*
[4]*AIR Division, National Physical Laboratory, Teddington TW11 0LW, United Kingdom*
[5]*Department of Physics, Faculty of Science, University of Zagreb, Bijenicka Cesta 32, HR-10000 Zagreb, Crotia*
[6]*Center for Computational Sciences, University of Tsukuba, Tsukuba 305-8577, Japan*
[7]*Institut für Kernphysik, T.U. Darmstadt, 64289 Darmstadt, Germany*
[8]*University of Bucharest, Faculty of Physics, Magurele-Bucharest, Romania*

(Received 20 December 2016; published 28 February 2017)

The properties of excited states in the neutron-rich nucleus ^{194}Os have been investigated using the ^{192}Os(^{18}O,^{16}O)^{194}Os reaction with an 80 MeV beam provided by the IFIN-HH Laboratory, Bucharest. Discrete γ-ray decays from excited states have been measured using the hybrid HPGe-LaBr$_3$(Ce) array RoSPHERE. The current work identifies a number of previously unreported low-lying nonyrast states in ^{194}Os as well as the first measurement of the half-life of the yrast 2^+ state of 302(50) ps. This is equivalent to a $B(E2:2^+ \rightarrow 0^+) = 45(16)$ W.u. and intrinsic quadrupole deformation of $\beta_{\text{eff}} = 0.14(1)$. The experimental results are compared with Hartree-Fock-Bogoliubov–interacting-boson-model calculations and are consistent with a reduction in a quadrupole collectivity in Os isotopes with increasing neutron number.

DOI: 10.1103/PhysRevC.95.024328

I. INTRODUCTION

Nuclear deformation away from sphericity in even-even nuclei can be studied from a simple perspective by using properties of the lowest lying spin/parity $I^\pi = 2^+$ excited state such as its excitation energy and electromagnetic decay transition probability. The ratio of the energies of the first spin/parity 4^+ to 2^+ states, $R_{(4/2)} = E(4^+)/E(2^+)$ can also be used to describe the degree of nuclear collectivity [1–3]. These experimental signatures describe shape evolution with changing nucleon number, where $R_{(4/2)} < 2.0$ is associated with nuclei near closed shells; $R_{(4/2)} \approx 2.0$ is consistent with quadrupole vibrational structures and $R_{(4/2)} \approx 3.33$ describes axially symmetric, quadrupole deformed rotational nuclei [3–6]. A value of $R_{(4/2)} \simeq 2.5$ is expected for a nonaxially symmetric or γ-soft rotor [5].

The discontinuity in the $R_{(4/2)}$ ratio trend at the $N = 116$ nucleus ^{190}W [7,8] has been suggested to be evidence of a phase transition between the prolate and oblate shapes [9] in this region. The structure of the neighboring nucleus ^{194}Os has been the focus of previous research in search of a transition from prolate to oblate shapes [10–17]. Bond and co-workers [16] described this nucleus as a pivotal point for shape transition from the lighter mass deformed isotopes to spherical structures close to the $N = 126$ magic core [14–16]. Wheldon *et al.* [11] predict in their total Routhian surfaces (TRS) calculations an evolution of structure from a γ-soft prolate ($\gamma = 0^\circ$) minimum at ^{190}Os to a well-deformed oblate shape for ^{196}Os$_{120}$ [11]. Isomer-delayed spectroscopy of the $N = 122$ isotone ^{198}Os is consistent with an oblate deformation for both the reported isomeric state and the lower-lying states through which it decays to the ground state [18]. Hartree-Fock calculations by Stevenson *et al.* [10] predict that as the $N = 126$ closure is approached, the magnitude of the deformation parameter β_2 decreases with near-equal depth prolate and oblate minimum at $N = 116$. The aim of the current work is to investigate the low-lying collectivity in ^{194}Os by measurement of nonyrast energy levels, together with the $B(E2:2_1^+ \rightarrow 0_{\text{g.s}}^+)$ and the corresponding β_2 value, to provide more detailed information on the low-lying, collective structures at the predicted prolate/oblate shape boundary.

II. EXPERIMENTAL DETAILS AND DATA ANALYSIS

The ^{194}Os nuclei of interest were formed following the bombardment of an enriched (∼99%) 20 mg/cm^2 ^{192}Os target with a 80 MeV ^{18}O beam. The typical on-target DC beam current was 20 pnA over 9 d. The beam interaction also produced a range of other residual nuclei following fusion evaporation on Si, Ca, and Fe target trace contaminant products. The observed reaction products were ^{42}Ca [6,19,20], ^{50}Cr [21–23], ^{51}Cr [24–26], ^{51}Mn [27,28], ^{54}Fe [29,30], ^{67}Ga [6,31], and ^{68}Ge [32,33].

Apart from the ^{194}Os obtained from the $2n$-transfer reaction and the contaminants channels from fusion on Ca, Cr, Mn, Fe, Ge, and Ga, fusion evaporation channels were also identified from the bombardment of the ^{192}Os target with the beam to form ^{205,206}Po [6,34,35] via the $5n$ and $4n$ evaporation channels, respectively. Excited states in the ^{192}Os target [36,37] were populated through unsafe Coulomb excitation of ^{192}Os by the ^{18}O beam.

*t.daniel@surrey.ac.uk

 ©2017 American Physical Society

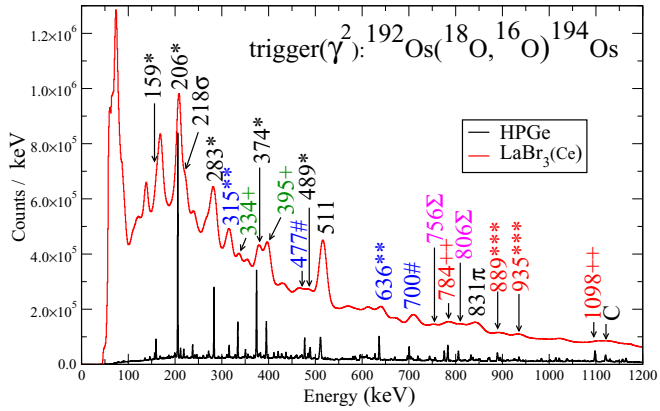

FIG. 1. Total projections of the HPGe and $LaBr_3(Ce)$ detectors with double prompt coincidence condition applied. Peaks identified with an asterisk are associated with ^{192}Os, $\sigma = {}^{194}$Os, $++ = {}^{50}$Cr, $\pi = {}^{51}$Mn, $\Sigma = {}^{54}$Fe, $\# = {}^{206}$Po, $+ = {}^{205}$Po, $*** = {}^{67}$Ga and C = contamination.

Reaction γ rays were identified using the RoSPHERE spectrometer [38] which comprised 14 HPGe detectors and 11 $LaBr_3(Ce)$ fast-timing detectors from the electronic 2 HPGe or 2 $LaBr_3(Ce)$ coincidence trigger condition. The data were sorted offline using different software coincidence conditions of double (γ^2) and triple (γ^3) prompt γ-ray coincidences (i.e., with a coincidence timing window of ± 50 ns) between either 2 HPGe or 2 $LaBr_3(Ce)$ scintillator detectors. Figure 1 shows the comparison of the total projections of the HPGe and LaBr3(Ce) detector types with the double gating hardware trigger condition applied.

III. LEVEL SCHEME FOR ^{194}Os

The excited states in ^{194}Os were populated through the ^{192}Os(^{18}O, ^{16}O) two-neutron transfer reaction. The level scheme of ^{194}Os as deduced in the current work is shown in Fig. 2. This is consistent with the previously reported results on the yrast 2_1^+ [11,12], 4_1^+, 6_1^+, 8_1^+, and 10_1^+ states [11], and the 2_2^+ excited state at 655-keV reported by Flynn *et al.* [39] and Casten *et al.* [12]. A total of 13 previously unreported γ-ray transitions were identified and placed into the level scheme in the current work (see Table I for details).

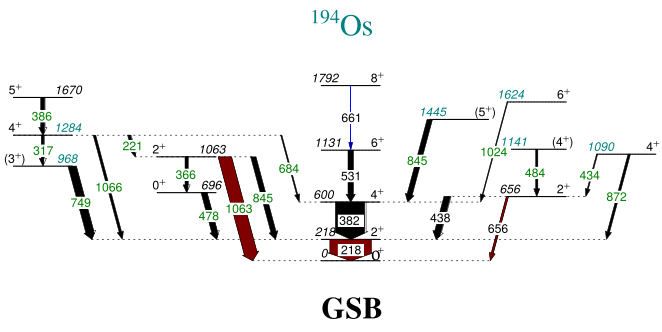

FIG. 2. The partial level scheme of ^{194}Os identified in the current study using the ^{192}Os(^{18}O, ^{16}O)^{194}Os reaction. The widths of the arrows indicate the observed relative γ-ray intensities.

TABLE I. The observed transitions associated with ^{194}Os in the current work. Newly observed and placed transitions are marked with a $^{\delta}$. Newly placed energy levels are marked with an asterisk. $E2$—quadrupole, $\Delta I = 1$—mixed $M1/E2$ or $E1$. Tentative spin/parity assignments are given in parentheses.

E_γ (keV)	I_γ (Rel.)	R_{DCO}	Multipolarity of transition	J_i^π	J_f^π	Transition $E_i \rightarrow E_f$
218	114		$E2$	2^+	0^+	$218 \rightarrow 0$
221^{δ}	10	1.0(6)	$E2$	$(3,4^+)$	2^+	$1284^* \rightarrow 1063$
317^{δ}	9	1.0(7)	$\Delta I = 1$	(4^+)	(3^+)	$1284^* \rightarrow 968$
366^{δ}	10	1.1(7)	$E2$	2^+	0^+	$1063 \rightarrow 696$
382	100	1.4(7)	$E2$	4^+	2^+	$601 \rightarrow 218$
386^{δ}	13	2(1)	$\Delta I = 1$	(5^+)	(4^+)	$1670 \rightarrow 1284$
434^{δ}	3	0.9(7)	$E2$	$(3,4^+)$	2^+	$1090^* \rightarrow 656$
438	22	1.5(8)	$\Delta I = 0$	2^+	2^+	$656 \rightarrow 218$
478^{δ}	20	1.2(7)	$E2$	0^+	2^+	$696 \rightarrow 218$
484^{δ}	7	0.9(6)	$E2$	(4^+)	2^+	$1141 \rightarrow 656$
531	18	1.4(8)	$E2$	6^+	4^+	$1131 \rightarrow 601$
656	7		$E2$	2^+	0^+	$656 \rightarrow 0$
661	$\leqslant 12$	1.9(8)	$E2$	8^+	6^+	$1792 \rightarrow 1131$
684^{δ}	4	0.5(5)	$\Delta I = 0$	(4^+)	4^+	$1284 \rightarrow 601$
749^{δ}	27	0.9(6)	$\Delta I = 1$	3	2^+	$968^* \rightarrow 218$
845^{δ}	18	1.0(6)	$\Delta I = 0$	2^+	2^+	$1063 \rightarrow 218$
872^{δ}	8	0.5(4)		$(3,4^+)$	2^+	$1090^* \rightarrow 218$
1024^{δ}	3	0.6(5)		$(5,6^+)$	4^+	$1624^* \rightarrow 601$
1063^{δ}	44		$E2$	2^+	0^+	$1063 \rightarrow 0$
1066^{δ}	8	0.7(6)		$(3,4^+)$	2^+	$1284^* \rightarrow 218$

Spin and parity assignments associated with these previously unreported states were made on the basis of γ-ray selection rules and the directional correlation of oriented states, (DCO) technique [40].

The relative intensities of the measured γ-ray energies in the current work were fitted using a HPGe gated HPGe projection with a gate on the 218-keV ($2^+ \rightarrow 0^+$) transition. The relative intensities of the 218-keV ($2^+ \rightarrow 0^+$), 1063-keV ($2_3^+ \rightarrow 0^+$), and 656-keV ($2_2^+ \rightarrow 0^+$) γ-ray energies were obtained using their relative intensities of the HPGe γ^2 total projection normalized to the intensity of the 382-keV ($4^+ \rightarrow 2^+$) transition in the same projection. The intensity of the 661-keV γ-ray energy is estimated to be $\leqslant 12\%$ of the 382-keV intensity. Table I presents the summary of the observed transitions associated with ^{194}Os as obtained in the current work.

Figure 3 shows the γ-ray spectra from data sorted with the γ-γ software trigger for gates on the 218 keV and 221 keV transitions in ^{194}Os. Apart from the stretched $E2$ transitions in the ground state band at 218 keV ($2_1^+ \rightarrow 0_1^+$), 382 keV ($4_1^+ \rightarrow 2_1^+$), 531 keV ($6_1^+ \rightarrow 4_1^+$) and 661 keV ($8_1^+ \rightarrow 6_1^+$) [11], and the 438 keV ($2_2^+ \rightarrow 2_1^+$), 656 keV ($2_2^+ \rightarrow 0_1^+$) [12] and 478 keV ($0^+ \rightarrow 2^+$) [41], all other identified transitions in the current work are reported for the first time. The 749 keV γ-ray transition was reported by Wheldon *et al.* as the ($10^+ \rightarrow 8^+$) populating the 1792 keV energy level from the 2541-keV level [11]. The current work observed the 749 keV transition as a

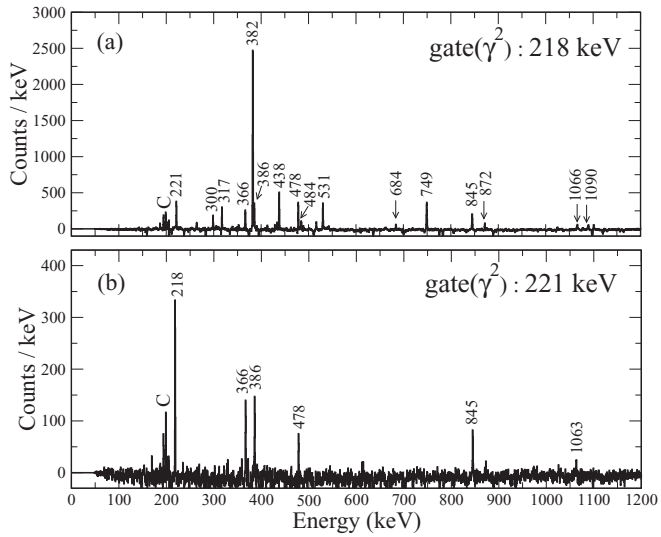

FIG. 3. Symmetrized background subtracted γ^2 coincidence gates on (a) the 218 and (b) 221 keV transitions showing γ-ray transitions associated with decays from excited states in ^{194}Os. Contaminant coincident transitions are labeled with C.

decay from the 968 keV $\rightarrow$ 218 keV levels which is not in coincidence with the 382 keV ground-state band transition.

The spin and parity of the yrast $I^\pi = 2^+,4^+,6^+$, and 8^+ states at $E_x = 218$, 600, 1131, and 1792 keV, respectively, in ^{194}Os has been established previously, assuming near-yrast feeding of the ground state band by Wheldon *et al.* [11]. Below we discuss the likely spin/parity assignments of the nonyrast states observed in the present work.

A. The 656 keV level

The 656 keV energy level is assigned spin/parity of 2_2^+ and decays by two transitions of 438 keV ($2_2^+ \rightarrow 2_1^+$) and 656 keV ($2_2^+ \rightarrow 0_{g.s}^+$). The level is fed by the 484 keV and 434 keV γ-ray transitions from the 1141 keV and 1090 keV energy levels, respectively. The $I^\pi = 2^+$ nature is established by this decay pattern and from the ^{192}Os$(t,p)^{194}$Os angular distribution data reported by Flynn and Burke [39].

B. The 696-keV level

The 696-keV level is fed by a 366-keV ($2_3^+ \rightarrow 0_2^+$) transition from the 1063 keV level. It decays directly to the $I^\pi = 2^+$ yrast 218 keV level by the 478 keV γ transition. There is no observed γ decay from the 696-keV state to the $I^\pi = 0^+$ ground state. Based on γ selection rules, the spin and parity assignment for the level in the current work are consistent with the $I^\pi = 0_2^+$ assignment provided by Flynn and Burke in their ^{192}Os$(t,p)^{194}$Os study [39].

C. The 968-keV level

There is no observed direct γ transition de-exciting to the 0_1^+ ground state nor to the 0_2^+ state. The only observed γ decay is to the yrast 2_1^+ state, which is consistent with γ-ray selection rules for an $M1$ and a (3^+) or an $E1$ and (3^-) assignment for this level. The state is fed by the decay from a proposed $(3,4_3^+)$ state at 1284 keV.

D. The 1063-keV level

The 1063-keV level decays by three discrete gamma transitions of energy 366-keV ($2_3^+ \rightarrow 0_2^+$), 1063 keV ($2_3^+ \rightarrow 0_1^+$), and 845 keV (i.e., $2_3^+ \rightarrow 2_1^+$). The $I^\pi = (2_3^+)$ assignment for the 1063 keV state is consistent with these allowed decay modes.

E. The 1090-keV level

The state is observed to decay via the 434 keV and 872 keV γ-ray transitions to the $I^\pi = 2_2^+$ and 2_1^+ excited states, respectively; however, no direct decay is observed to the 4_1^+ at 600 keV. There is also no observed gamma decay directly to the 0_1^+ ground state, although a 0^+ assignment cannot be ruled out. This state was not observed in the (t,p) study by Flynn and Burke which gives a preference for the higher spin (4^+) assignment, 3^+ or 3^- also possible.

F. The 1141-keV level

The 1141 keV state decays via a 484-keV transition to the 2_2^+, with no competing observed decay to the 0_1^+ ground state. The DCO ratio of 0.9(6) is consistent with a stretched $E2$ transition for the 484 keV γ ray and a tentative $I^\pi = (4^+)$ assignment for this state. No decay is observed from this state to the yrast 2^+ state at 218 keV.

G. The 1284-keV level

The decay via 317-keV to the 968-keV level most likely has a mixed dipole/quadrupole ($M1/E2$) multipolarity. The spin and parity assignment of 4^+ is favored since there is no observed decay from the 1284-keV energy level directly to the 0_1^+ ground state or the 0_2^+ state of the 696-keV energy level, but direct decays are observed to the $I^\pi = 2_1^+$ (218 keV), 4_1^+ (600 keV) states and 2^+ state at 1063 keV. A spin assignment of (3) cannot be definitively ruled out but $I^\pi = 4^+$ is preferred.

H. The 1624-keV level

The γ decay out of the 1624 keV energy state to the $I^\pi = 4^+$, 600 keV state observed in the current work is assigned as a stretched $E2$ transition. No other γ decays were observed from this state. The spin and parity assignment of (6^+) for the state suggests other possible $E2$ decays to the 1141-keV and 1090-keV $I^\pi = 4^+$ states would be possible, but these were not observed in the current work. A spin 5 assignment cannot be ruled out.

I. The 1670-keV level

Only a single γ-ray transition at 386 keV is observed from this state. The DCO ratio is consistent with a mixed $M1/E2$, $\Delta I = 1$ transition and as such, a spin and parity assignment of (5^+) is favored on the basis of near-yrast feeding. This is consistent with the γ-ray selection rules since there is no observed decay to the 1063-keV $I^\pi = 2_3^+$ level or other 2^+

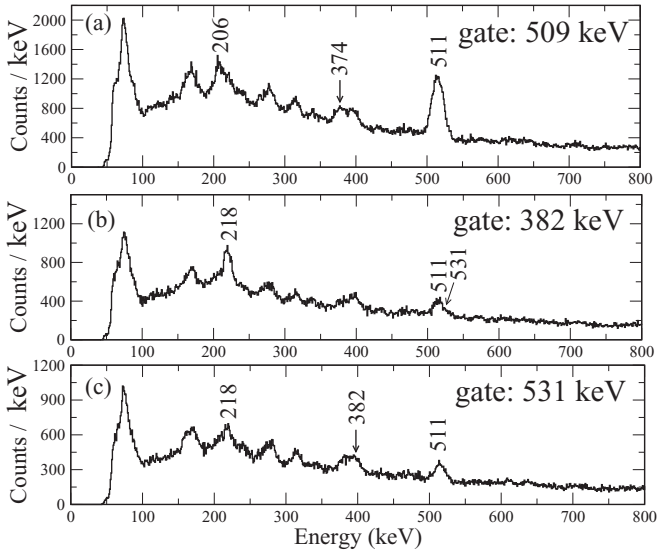

FIG. 4. (a) 509 keV HPGe gate showing the 206 and 374 keV transitions in the ^{192}Os ground state band on $LaBr_3$(Ce)-$LaBr_3$(Ce) projections. (b) $LaBr_3$(Ce) projection gated in the 382 keV $4^+ \rightarrow 2^+$ transition in ^{194}Os in the HPGe detectors showing the coincident transitions at 218 keV and 531 keV. (c) HPGe gated on the 531 keV $6^+ \rightarrow 4^+$ transition in ^{194}Os, showing the coincident 218 keV and 382 keV transitions.

states at 218 keV and 656 keV. A state of energy 1668 keV was reported by Flynn and Burke in their (t, p) study, but no spin/parity assignment was made.

IV. HALF-LIFE MEASUREMENT OF THE YRAST $I^\pi = 2^+$ EXCITED STATE IN ^{192,194}Os

Prior to the half-life measurement of the yrast $I^\pi = 2^+$ in ^{194}Os, an internal check of the analysis procedure was performed using the reported half-life value of 288(4) ps [42] for the yrast $I^\pi = 2^+$ state in ^{192}Os. This was measured in the current work as the time difference between the 206 and 374 keV ground state band transitions. Figure 4(a) shows the effects of single gates on the HPGe detectors for selection of this cascade using a gate on the 509 keV $6^+ \rightarrow 4^+$ transition in ^{192}Os in the HPGe detectors. Figures 4(b) and 4(c) show analogous gates set on the 382 keV and 531 keV transitions in ^{194}Os.

The upper panel of Fig. 5 shows a background subtracted single 206 keV gate in the $LaBr_3$-$LaBr_3$ energy coincidence matrix while the lower panel shows the spectrum resulting from a background-subtracted gate on the γ-ray coincident partner transition at 374 keV. These energy gates were used to extract the time difference between the 206 keV and 374 keV transitions for the yrast $I^\pi = 2^+$ state in ^{192}Os. The three-dimensional background subtraction to generate the final time difference spectrum is described by Werner *et al.* in [43].

The half-life for the yrast $I^\pi = 2^+$ state in ^{194}Os was determined by using the HPGe gated, $LaBr_3$(Ce)-$LaBr_3$(Ce) coincidences with a 531-keV $I^\pi = 6^+ \rightarrow 4^+$ gate on the HPGe detectors and a projection of the time differences between the 218 keV γ-ray transition and the peak and Compton

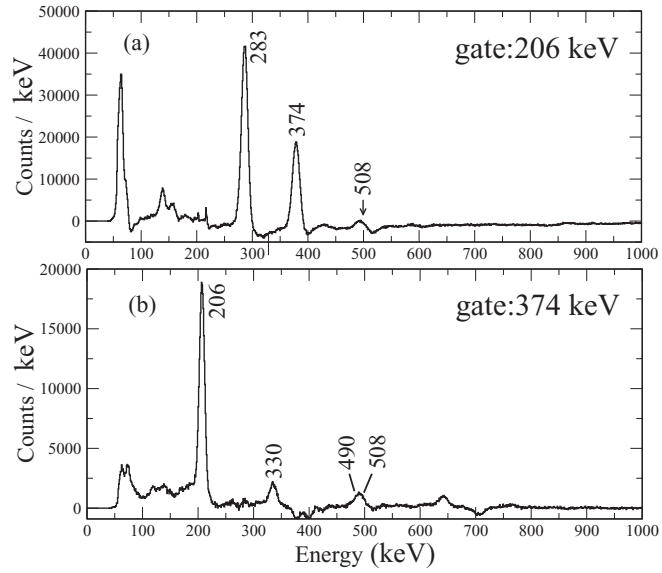

FIG. 5. Symmetrized $LaBr_3$(Ce) γ-γ matrix showing background-subtracted gates on (a) the 206 keV and (b) 374 keV transitions in ^{192}Os, which were used for the extraction of the time difference between these two transitions.

transitions associated with the 382 keV transition (see details in Fig. 6). By using HPGe–$LaBr_3$(Ce)-$LaBr_3$(Ce) coincidences, a 531 keV HPGe gate was imposed a $E_{\gamma 1}$–$E_{\gamma 2}$-ΔT cube.

Figure 7(a) shows the background-subtracted time difference between the coincidence pair of 206 keV and 374 keV. The resulting half-life value obtained from the deconvoluted fit to this spectrum is 284(16) ps. This fit used a fixed Gaussian

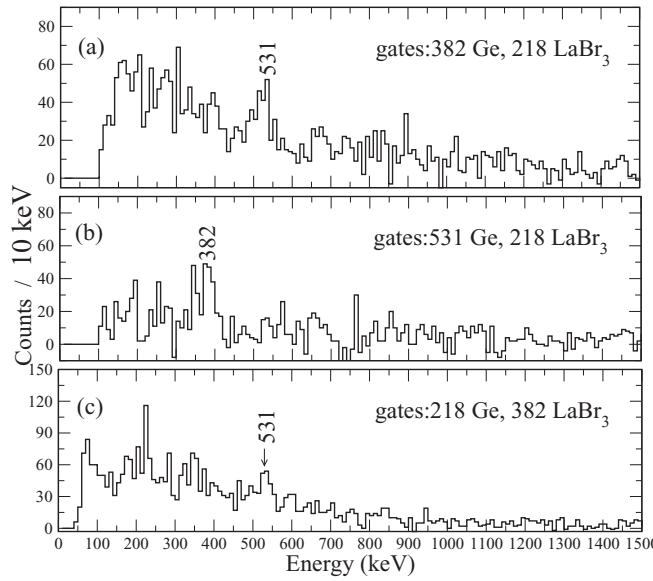

FIG. 6. Double gates on transitions in ^{194}Os. (a) The $LaBr_3$(Ce) projections showing the coincident 531 keV from the effect of the 382 keV HPGe gate and 218 keV $LaBr_3$(Ce) gate. (b) Double gates on the 531 keV HPGe and 218 keV $LaBr_3$(Ce) showing the coincident 382 keV transition in the $LaBr_3$(Ce) detectors. (c) Double gates on the 218 keV HPGe and 382 keV $LaBr_3$(Ce) showing the coincident 531 keV $LaBr_3$(Ce) transition.

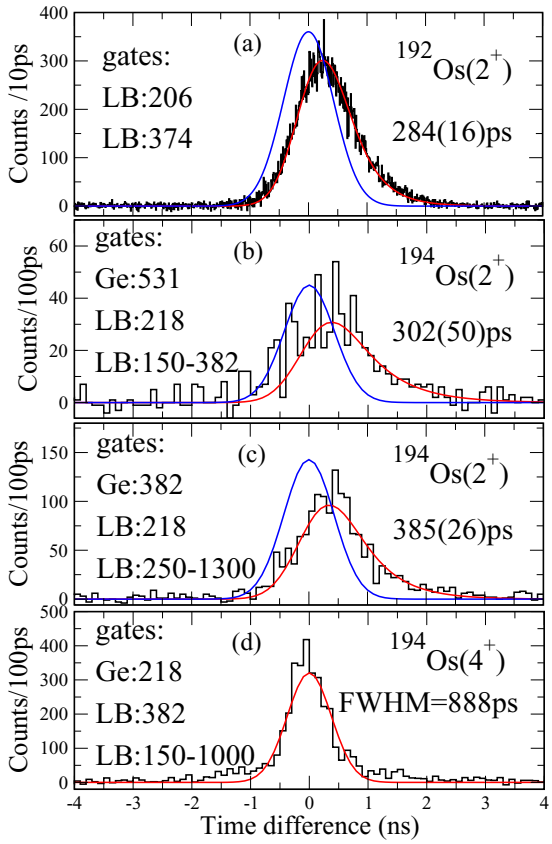

FIG. 7. (a) Background subtracted time difference spectra for the yrast $I^\pi = 2^+$ state in ^{192}Os, obtained from the $LaBr_3$(Ce) $E_{\gamma 1}$-$E_{\gamma 2}$-ΔT cube, showing the time difference between the 206 and 374 keV γ-ray pairs. A PRF with a FWHM = 1007 ps (shown in blue) was used in this fit. (b) Time difference with a HPGe gate on 531 keV $6^+ \rightarrow 4^+$ γ ray in ^{194}Os between the 218 keV and 150–382 keV $LaBr_3$(Ce) transitions used to isolate the lifetime of the 2^+ state in ^{194}Os. A PRF with a FWHM = 1007 ps was also used in this fit. (c) Time difference with a HPGe gate on 382 keV γ-ray between the 218 keV and 250-1300 keV $LaBr_3$(Ce) transitions in ^{194}Os. A PRF with a FWHM = 1007 ps was used in this fit. (d) Time difference with a HPGe gate on 218 keV γ energy between the 382 keV and 150–1000 keV $LaBr_3$(Ce) transitions in ^{194}Os to isolate the apparent half-life of the $I^\pi = 4^+$ state in ^{194}Os. The prompt response fit for this time-difference spectra is 888 ps.

prompt-response function value of FWHM = 1007 ps which was obtained from the ΔT between the Compton γ pairs of the 189 keV and 237 keV transitions. This values are consistent with the evaluated value for the yrast $I^\pi = 2^+$ state in ^{192}Os of 288(4) ps [42].

The time difference spectra between the $LaBr_3$(Ce) detectors gated on the coincident energies of 218 keV and γ-ray energies between 150 and 382 keV (i.e., the 382 keV full-energy peak and the associated Compton events) were then projected. Figure 7(b) presents the extracted half-life value of 302(50) ps for the yrast 2^+ state in ^{194}Os. This value was obtained using a least squares fit and χ squared minimization for the fitted half-life, assuming a fixed, Gaussian prompt response function FWHM = 1007 ps. This value of the half-life corresponds to a $B(E2 : 2^+ \rightarrow 0^+) = 0.30(4)\ e^2b^2$.

TABLE II. The calculated $B(E2 : 2^+ \rightarrow 0^+)$ and the intrinsic quadrupole deformation parameter, $\beta_{\rm eff}$, values from the extracted half-life value = 302(50) ps for the yrast $I^\pi = 2^+$ state in ^{194}Os. The value of the total internal conversion coefficient α is obtained from BRICC [44].

E_γ (keV)	$I_i^\pi \rightarrow I_f^\pi$	HPGe (gate)	ICC α	$T_{1/2}$ (ps)	$B(E2)$ (W.u.)	$B(E2)$ (e^2b^2)	$\beta_{\rm eff}$
218	$2^+ \rightarrow 0_1^+$	531	0.249(4)	302(50)	45(16)	0.30(4)	0.140(10)

V. DISCUSSION

Assuming axial symmetry, the extracted half-life of the yrast 2^+ state in ^{194}Os can be used to determine a value for the effective quadrupole deformation parameter (see Table II) using equation 1 [45,46], which relates the $B(E2 : 0^+ \rightarrow 2^+)$ to the β_2 deformation parameter [47–49]. This can then be related to the *effective* quadrupole deformation parameter $\beta_{\rm eff}$ through the use of shape invariants [50] to the $B(E2 : 0^+ \rightarrow 2^+)$ value by

$$\beta_2 \approx \beta_{\rm eff} = \left(4\pi/3ZR_0^2\right)[B(E2;0^+ \rightarrow 2_1^+)/e^2]^{1/2}, \qquad (1)$$

where $R_0 = 1.2 \times 10^{-13} A^{1/3}$cm $= (1.2A^{1/3})$fm is the average radius of the nucleus and $B(E2;0^+ \rightarrow 2_1^+)$ in e^2b^2 is the reduced transition probability for the $E2$ transition [$= B(E2 : 2^+ \rightarrow 0^+) \times 5$].

The calculated quadrupole deformation parameter of $|\beta_{\rm eff}| = 0.140(10)$ for the yrast 2^+ state in ^{194}Os is consistent with the total Routhian surface calculations by Wheldon *et al.* [11]; which predict a shallow prolate deformed minimum with $\beta_2 = 0.16$. The experimental value is also consistent with the recent predictions using the PES method by Wang *et al.* [51] of $\beta_2 = 0.127$. The Hartree-Fock calculations by Nazarewicz *et al.* [17] predict a ground state oblate deformation for ^{194}Os of $\beta_2 = -0.14$, with a change of prolate to oblate shape going from ^{192}Os $\rightarrow$ ^{194}Os.

A. Energy systematics in ^{194}Os and other osmium isotopes for N = 100–122

Figure 8 presents systematics of the yrast $I^\pi = 2^+,4^+,6^+,8^+$ excited states in ^{194}Os and other osmium isotopes for neutron numbers N = 100–122 together with the first excited 0_2^+ and the second 2_2^+ states. The $E(2_1^+)$ for the osmium isotopes increases from $N = 108$ until $N = 118$, followed by a more dramatic change from $N = 120 \rightarrow 122$, as the magic number at $N = 126$ is approached. A similar reduction in collectivity is indicated by the related increase in the energies of the yrast states with $I^\pi = 4^+,6^+$ and 8^+ as N increases from $N = 108$ to 122. There is a decrease in the energy of the yrast states around $N = 108$, which is four neutrons away from the midshell at $N = 104$, implying a maximum quadrupole deformation for the Os isotopes at this neutron number.

The excitation energy of the $I^\pi = 2_2^+$ is observed to decrease from $N = 108$ up to $N = 116$ followed by a notable increase for the heavier osmium isotopes including $^{194}Os_{118}$. The increase in the excitation energy of the $I^\pi = 2_2^+$ at

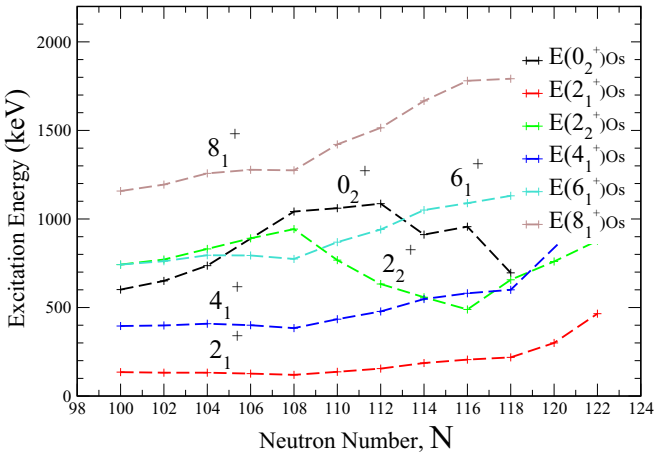

FIG. 8. Systematics of the ground state band $E(2_1^+)$, $E(4_1^+), E(6_1^+), E(8_1^+)$ and $E(0_2^+), E(2_2^+)$ for Os isotopes with $N =$ 100–122.

$N \geqslant 118$ is consistent with the prediction of shape changes from the deformed prolate configuration in lighter isotopes to a weakly oblate configuration for $N \geqslant 118$ [10–12,16,17,41] across the maximum of γ softness at $N = 116$.

The excitation energy of the first excited 0_2^+ state has a minimum energy of 696 keV at $N = 118$, as confirmed in the current work and the in work of Al-Dahan and co-workers [41]. This excitation energy, together with those of the $E(2_2^+) =$ 656.54 keV and $E(4_1^+) = 600$ keV in ^{194}Os are consistent with an anharmonic vibrational picture with this triplet of states lying at ∼2.5 times the energy of the first $2^+ = 218$ keV state [1].

B. Quadrupole collectivity across the W-Pt isotopic chains

The systematic plots of the $B(E2 : 0^+ \rightarrow 2^+)$ and the associated intrinsic quadrupole deformation parameter, β_{eff}, values for Os ($Z = 76$), W ($Z = 74$), and Pt ($Z = 78$) isotopes with $N =$ 100–120 are shown in Fig. 9. As expected, there is a decreasing trend in the $B(E2 : 0^+ \rightarrow 2^+)$ and the corresponding β_{eff} values, as N approaches $N = 126$. The systematics of $B(E2 : 0^+ \rightarrow 2^+)$ values and the β_{eff} values at $N = 118$ show a larger decrease for ^{194}Os, compared to the trend in the lighter Os isotopes. By comparing with the neighboring even-even W and Pt isotopic chains, the systematics of $B(E2 : 0^+ \rightarrow 2^+)$ and β_{eff} values in the W-Pt isotopic chain, show a decrease up to N = 116, as N increases from N = 106-116. Beyond the N = 116, the Os isotopes decrease more rapidly in both the $B(E2 : 0^+ \rightarrow 2^+)$ and β_{eff} values at $N = 118$, consistent with a transition to a less deformed (possibly oblate) configuration as the neutron magic number at $N = 126$ is approached.

C. Comparison with the IBM calculations

Figure 10 compares the energy level scheme of ^{194}Os from the current work to that of the prediction using the interacting boson model (IBM) by Nomura *et al.* [13]. The energy spacing in the ground state rotational band structure from this work is

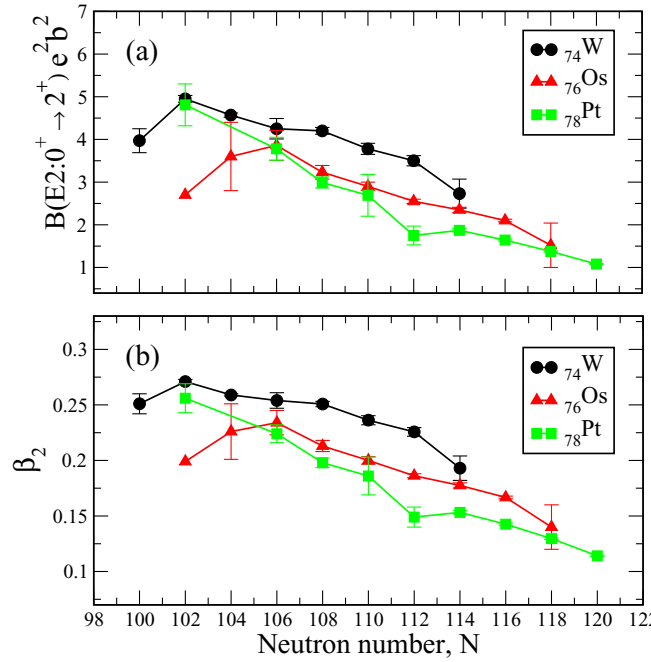

FIG. 9. Systematics of (a) $B(E2 : 0^+ \rightarrow 2^+)$ and (b) $\beta_{\text{eff}} \approx \beta_2$ values for tungsten (W), osmium (Os), and platinum (Pt) isotopes. Data points are taken from Refs. [47,48] except the $B(E2 : 0^+ \rightarrow 2^+)$ for ^{174,180,}W, ^{178}Os, ^{182}Pt [52], ^{176}W [53], ^{178}W [54], and ^{188}W [55]. The $B(E2 : 0^+ \rightarrow 2^+)$ value for ^{194}Os ($N = 118$) is from the current work.

reasonably well reproduced by the IBM calculations, with the experimental energies of the respective levels, up to the yrast $I^\pi = 4^+$ state consistent with those generated by the IBM. The level energy differences are more pronounced from the yrast $I^\pi = 6^+$ state with 1131 keV in the current work compressed compared to the predicted 1334 keV by the IBM, while the yrast 8^+ state has 1792 keV compares to the 2182 keV by the IBM.

The $I^\pi = 2_2^+$ state at an excitation energy of 656 keV in the current work is about ∼200 keV lower than the predicted state (865 keV) by the IBM [13]. While candidates for both the quasi-γ-bandhead (2_γ^+) at 656 keV, and the quasi-β-bandhead (0_2^+) at 696 keV can be identified in the current work, both are considerably lower in energy in the experimental data compared to the IBM predicted values of 865 keV and 1456 keV, respectively. Nomura and co-workers [13] interpreted the level energy difference as an evidence for γ instability with a predicted $B(E2 : 2_2^+ \rightarrow 2_1^+)/B(E2 : 2_1^+ \rightarrow 0_1^+)$ ratio close to the O(6) limit in ^{194}Os. As presented in Fig. 10, the predicted energy staggering in the proposed γ band is not well reproduced in the current work. The predicted (mixed symmetry) excited states with spin/parity 1_1^+ at 1960 keV and 3_2^+ at 2052 keV energies are not observed. In general, the experimental levels are more compressed compared to the IBM calculations. In the IBM based theoretical calculations the effective charges were chosen to fit the measured $B(E2 : 2^+ \rightarrow 0^+)$ in ^{192}Os. The theoretical transition strength for ^{194}Os is $B(E2 : 2^+ \rightarrow 0^+) = 0.33\ e^2b^2$. This is in agreement with the experimentally obtained value of 0.30(4) e^2b^2

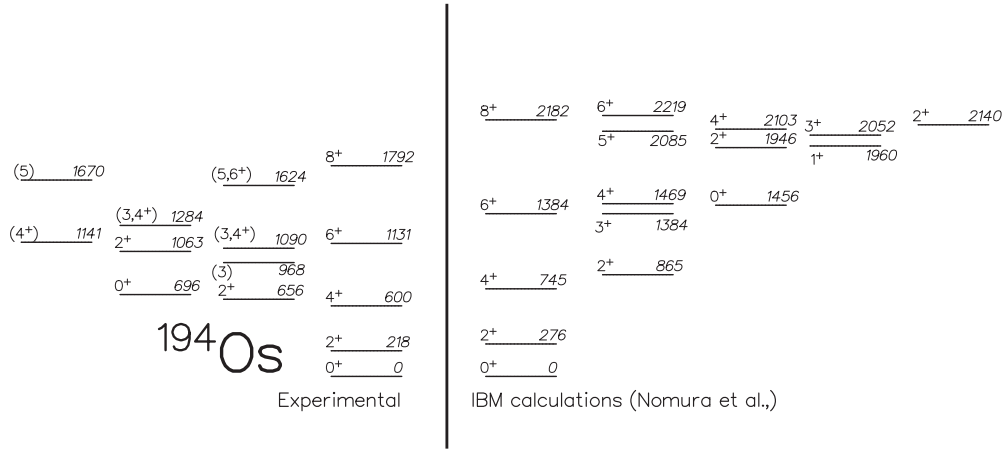

FIG. 10. The level schemes of the low-lying levels in ^{194}Os showing comparison between the IBM calculations of Nomura *et al.* [13] and the experimental data in the current work.

obtained in the current work. The calculation correctly predict the decrease in transition strength in ^{194}Os when compared to ^{192}Os.

VI. SUMMARY AND CONCLUSIONS

A number of previously unreported nonyrast states in the neutron-rich nucleus ^{194}Os have been reported in the current work. γ-ray transitions together with their relative intensities are reported for]decays associated with the first excited spin/parity 0^+ and 2^+ states together with candidates for a number of other nonyrast low-lying collective states in this nucleus. The electromagnetic transition probability for the decay from the yrast spin/parity 2^+ state to the ground states has been measured using fast-timing electronic coincidence spectroscopy. The resulting half-life of 302(50) ps is used to infer an effective quadrupole deformation for the first 2^+ transition in this nucleus of $\beta_{\text{eff}} = 0.14$ which is consistent with the prediction of a steady decrease in deformation across the Os isotopic chain with increasing neutron number from the $N = 104$ midshell towards the spherical shell closure at $N = 126$.

ACKNOWLEDGMENTS

We would like to thank the staff of IFIN-HH, Romania for their support during this experiment and Paul Morrall of the Daresbury Laboratory UK for making of the ^{192}Os target. This work was supported by The Science and Technology Facilities Council UK by Grant No. ST/L005743/1. P.H.R. acknowledges partial support from the UK National Measurement Office (NMO). K.N. acknowledges support from the Japan Society for the Promotion of Science and by the QuantiXLie Center of Excellence. This work was partially supported by the Romanian Grant No. PNIII-IFA-FAIR-NUSTAR-RO. C.R.N. would like to acknowledge the support from the PN-II-RU-TE-2014-4-2003 and NUSTAR 03 FAIR projects. T.D. would also like to acknowledge the PhD sponsorship from TeTfund/BSU Makurdi, Nigeria.

[1] K. S. Krane, *Introductory Nuclear Physics*, revised edition (John Wiley and Sons, Inc., New York, 1988).
[2] I. Ragnarsson and R. K. Sheline, Phys. Scr. **29**, 385 (1984).
[3] R. B. Cakirli and R. F. Casten, Phys. Rev. C **78**, 041301(R) (2008).
[4] G. Sharff-Goldhaber and J. Weneser, Phys. Rev. **98**, 212 (1955).
[5] R. F. Casten, Phys. Lett. B **152**, 145 (1985).
[6] Evaluated Nuclear Structure Data File (ENSDF), http://www.nndc.bnl.gov/ensdf/; retrieved 2016.
[7] Zs. Podolyák, P. H. Regan, M. Pfützner, J. Gerl, M. Hellström, M. Caamaño, P. Mayet, Ch. Schlegel, A. Aprahamian, J. Benlliure, A. M. Bruce, P. A. Butler, D. Cortina Gil, D. M. Cullen, J. Döring, T. Enqvist, F. Rejmund, C. Fox, J. Garcés Narro, H. Geissel, W. Gelletly, J. Giovinazzo, M. Górska, H. Grawe, R. Grzywacz, A. Kleinböhl, W. Korten, M. Lewitowicz, R. Lucas, H. Mach, M. Mineva, C. D. O'Leary, F. De Oliveira, C. J. Pearson, M. Rejmund, M. Sawicka, H. Schaffner, K. Schmidt, Ch. Theisen, P. M. Walker, D. D. Warner, C. Wheldon, H. J. Wollersheim, S. C. Wooding, and F. R. Xu, Phys. Lett. B **491**, 225 (2000).
[8] P. M. Walker and F. R. Xu, Phys. Lett. B **635**, 286 (2006).
[9] Y. Sun, P. M. Walker, Fu-Rong Xu, and Yu-Xin Liu, Phys. Lett. B **659**, 165 (2008).
[10] P. D. Stevenson, M. P. Brine, Zs. Podolyák, P. H. Regan, P. M. Walker, and J. R. Stone, Phys. Rev. C **72**, 047303 (2005).
[11] C. Wheldon, J. Garcés Narro, C. J. Pearson, P. H. Regan, Zs. Podolyák, D. D. Warner, P. Fallon, A. O. Macchiavelli, and M. Cromaz, Phys. Rev. C **63**, 011304(R) (2000).
[12] R. F. Casten, A. I. Namenson, W. F. Davidson, D. D. Warner, and H. G. Borner, Phys. Lett. B **76**, 280 (1978).

[13] K. Nomura, T. Otsuka, R. Rodríguez-Guzmán, L. M. Robledo, P. Sarriguren, P. H. Regan, P. D. Stevenson, and Zs. Podolyák, Phys. Rev. C **83**, 054303 (2011).

[14] K. Nomura, T. Otsuka, R. Rodríguez-Guzmán, L. M. Robledo, and P. Sarriguren, Phys. Rev. C **84**, 054316 (2011).

[15] P. Sarriguren, R. Rodríguez-Guzmán, and L. M. Robledo, Phys. Rev. C **77**, 064322 (2008).

[16] P. D. Bond, R. F. Casten, D. D. Warner, and D. Horn, Phys. Lett. B **130**, 167 (1983).

[17] W. Nazarewicz, M. A. Riley, and J. D. Garrett, Nucl. Phys. A **512**, 61 (1990).

[18] Zs. Podolyák, S. J. Steer, S. Pietri, F. R. Xu, H. L. Liu, P. H. Regan, D. Rudolph, A. B. Garnsworthy, R. Hoischen, M. Górska, J. Gerl, H. J. Wollersheim, T. Kurtukian-Nieto, G. Benzoni, T. Shizuma, F. Becker, P. Bednarczyk, L. Caceres, P. Doornenbal, H. Geissel, J. Grebosz, A. Kelic, I. Kojouharov, N. Kurz, F. Montes, W. Prokopowicz, T. Saito *et al.*, Phys. Rev. C **79**, 031305(R) (2009).

[19] E. K. Warburton, J. J. Kolata, and J. W. Olness, Phys. Rev. C **11**, 700 (1975).

[20] P. Herges, H. V. Klapdor, and T. Oda, Nucl. Phys. A **372**, 253 (1981).

[21] J. A. Cameron, J. L. Rodriguez, J. Jonkman, G. Hackman, S. M. Mullins, C. E. Svensson, J. C. Waddington, L. Yao, T. E. Drake, M. Cromaz, J. H. DeGraaf, G. Zwartz, H. R. Andrews, G. Ball, A. Galindo-Uribarri, V. P. Janzen, D. C. Radford, and D. Ward, Phys. Rev. C **58**, 808 (1998).

[22] F. Brandolini, S. M. Lenzi, D. R. Napoli, R. V. Ribas, H. Somacal, C. A. Ur, D. Bazzacco, J. A. Cameron, G. de Angelis, M. De Poli, C. Fahlander, A. Gadea, S. Lunardi, G. Martínez-Pinedo, N. H. Medina, C. Rossi Alvarez, J. Sánchez-Solano, and C. E. Svensson, Nucl. Phys. A **642**, 387 (1998).

[23] F. Brandolini, J. Sanchez-Solano, S. M. Lenzi, N. H. Medina, A. Poves, C. A. Ur, D. Bazzacco, G. De Angelis, M. De Poli, E. Farnea, A. Gadea, D. R. Napoli, and C. Rossi-Alvarez, Phys. Rev. C **66**, 021302(R) (2002).

[24] J. A. Cameron, D. G. Popescu, and J. C. Waddington, Phys. Rev. C **44**, 2358 (1991).

[25] D. G. Sarantites and W. G. Winn, Nucl. Phys. A **155**, 257 (1970).

[26] Z. P. Sawa and J. Blomqvist, Nucl. Phys. A **205**, 257 (1973).

[27] J. W. Noe, R. W. Zurmuhle, and D. P. Balamuth, Nucl. Phys. A **277**, 137 (1977).

[28] J. Ekman, C. Andreoiu, C. Fahlander, M. N. Mineva, D. Rudolph, M. A. Bentley, S. J. Williams, R. J. Charity, E. Ideguchi, W. Reviol, D. G. Sarantites, V. Tomov, R. M. Clark, M. Cromaz, P. Fallon, A. O. Macchiavelli, M. P. Carpenter, and D. Seweryniak, Phys. Rev. C **70**, 057305 (2004).

[29] J. Styczen, E. Bozek, T. Pawlat, Zb. Stachura, F. A. Beck, C. Gehringer, B. Haas, J. C. Merdinger, N. Schulz, P. Taras, M. Toulemonde, J. P. Vivien, and A. Müller-Arnke, Nucl. Phys. A **327**, 295 (1979).

[30] R. W. Benjamin and I. L. Morgan, Phys. Rev. **163**, 1252 (1967).

[31] V. Zobel, L. Cleemann, J. Eberth, W. Neumann, and N. Weihl, Nucl. Phys. A **316**, 165 (1979).

[32] D. Ward, C. E. Svensson, I. Ragnarsson, C. Baktash, M. A. Bentley, J. A. Cameron, M. P. Carpenter, R. M. Clark, M. Cromaz, M. A. Deleplanque, M. Devlin, R. M. Diamond, P. Fallon, S. Flibotte, A. Galindo-Uribarri, D. S. Haslip, R. V. F. Janssens, T. Lampman, G. J. Lane, I. Y. Lee, F. Lerma, A. O. Macchiavelli, S. D. Paul, D. Radford, D. Rudolph, D. G. Sarantites, B. Schaly, D. Seweryniak, F. S. Stephens, O. Thelen, K. Vetter, J. C. Waddington, J. N. Wilson, and C.-H. Yu, Phys. Rev. C **63**, 014301 (2000).

[33] A. P. de Lima, A. V. Ramayya, J. H. Hamilton, B. Van Nooijen, R. M. Ronningen, H. Kawakami, R. B. Piercey, E. de Lima, R. L. Robinson, H. J. Kim, L. K. Peker, F. A. Rickey, R. Popli, A. J. Caffrey, and J. C. Wells, Phys. Rev. C **23**, 213 (1981).

[34] V. Rahkonen, B. Fant, C. J. Herrlander, K. Honkanen, A. Källberg, and T. Weckström, Nucl. Phys. A **441**, 11 (1985).

[35] A. M. Baxter, A. P. Byrne, G. D. Dracoulis, R. A. Bark, F. Riess, A. E. Stuchbery, M. C. Kruse, and A. R. Poletti, Nucl. Phys. A **515**, 493 (1990).

[36] E. W. Kleppinger and S. W. Yates, Phys. Rev. C **27**, 2608 (1983).

[37] R. F. Casten, H. G. Börner, J. A. Pinston, and W. F. Davidson, Nucl. Phys. A **309**, 477 (1978).

[38] D. Bucurescu, I. Cãta-Danil, G. Ciocan, C. Costache, D. Deleanu, R. Dima, D. Filipescu, N. Florea, D. G. Ghiţa, T. Glodariu, M. Ivaşcu, R. Licã, N. Mãrginean, R. Mãrginean, C. Mihai, A. Negret *et al.*, Nucl. Instrum. Methods Phys. Res. A **837**, 1 (2016).

[39] E. R. Flynn and D. G. Burke, Phys. Rev. C **17**, 501 (1978).

[40] A. Kramer-Flecken, T. Morek, R. M. Lieder, W. Gast, G. Hebbinghaus, H. M. Jäger, and W. Urban, Nucl. Instrum. Methods Phys. Res. A **275**, 333 (1989).

[41] N. Al-Dahan, P. H. Regan, Zs. Podolyák, P. M. Walker, N. Alkhomashi, G. D. Dracoulis, G. Farrelly, J. Benlliure, S. B. Pietri, R. F. Casten, P. D. Stevenson, W. Gelletly, S. J. Steer, A. B. Garnsworthy, E. Casarejos *et al.*, Phys. Rev. C **85**, 034301 (2012).

[42] C. M. Baglin, Nucl. Data Sheets **113**, 1871 (2012).

[43] V. Werner, N. Cooper, J.-M. Régis, M. Rudigier, E. Williams, J. Jolie, R. B. Cakirli, R. F. Casten, T. Ahn, V. Anagnostatou, Z. Berant, M. Bonett-Matiz, M. Elvers, A. Heinz, G. Ilie, D. Radeck, D. Savran, and M. K. Smith, Phys. Rev. C **93**, 034323 (2016).

[44] T. Kibedi *et al.*, Nucl. Instrum. Methods Phys. Res. A **589**, 202 (2008).

[45] A. Bohr and B. R. Mottleson, *Nuclear Structure, Volume I: Nuclear Deformations* (World Scientific, Singapore, 1998).

[46] Y. Oktem, D. L. Balabanski, B. Akkus, L. A. Susam, L. Atanasova, C. W. Beausang, R. B. Cakirli, R. F. Casten, M. Danchev, M. Djongolov, E. Ganioğlu *et al.*, Phys. Rev. C **86**, 054305 (2012).

[47] S. Raman, C. W. Nestor, Jr., and P. Tikkanen, At. Data Nucl. Data Tables **78**, 1 (2001).

[48] B. Pritychenko, M. Birch, B. Singh, and M. Horoi, At. Data Nucl. Data Tables **107**, 1 (2016).

[49] I. Boboshin, B. Ishkhanov, S. Komarov, V. Orlin, N. Peskov, and V. Varlamov, Int'l Conf. Nucl. Data for Sci. and Tech. **65**, (2007).

[50] V. Werner, N. Pietralla, P. von Brentano, R. F. Casten, and R. V. Jolos, Phys. Rev. C **61**, 021301(R) (2000).

[51] H.-L. Wang, S. Zhang, M.-L. Liu, and F.-R. Xu, Prog. Theor. Exp. Phys. **2015**, 073D03 (2015).

[52] B. A. Bian, Y.-M. Di, G.-L. Long, Y. Sun, J. Y. Zhang, and J. A. Sheikh, Phys. Rev. C **75**, 014312 (2007).

[53] J.-M. Régis, Th. Materna, S. Christen, C. Bernards, N. Braun, G. Breuer, Ch. Fransen, S. Heinze, J. Jolie, T. Meersschaut, G. Pascovici, M. Rudigier *et al.*, Nucl. Instrum. Methods Phys. Res. A **606**, 466 (2009).

[54] M. Rudigier, J.-M. Régis, J. Jolie, K. O. Zell, and C. Fransen, Nucl. Phys. A **847**, 89 (2010).

[55] P. J. R. Mason, Zs. Podolyák, N. Mărginean, P. H. Regan, P. D. Stevenson, V. Werner, T. Alexander, A. Algora, T. Alharbi, M. Bowry, R. Britton, A. M. Bruce, D. Bucurescu, M. Bunce, G. Căta-Danil, I. Căta-Danil, N. Cooper, D. Deleanu, D. Delion, D. Filipescu, W. Gelletly, D. Ghiţă, I. Gheorghe, T. Glodariu, G. Ilie, D. Ivanova, S. Kisyov, S. Lalkovski, R. Lica, S. N. Liddick, R. Mărginean, C. Mihai, K. Mulholland, C. R. Nita, A. Negret, S. Pascu, S. Rice, O. J. Roberts, T. Sava, J. F. Smith, P.-A. Söderström, L. Stroe, G. Suliman, R. Suvaila, S. Toma, C. Townsley, E. Wilson, R. T. Wood, M. Zhekova, and C. Zhou, Phys. Rev. C **88**, 044301 (2013).